DC BUS VOLTAGE CONTROL FOR RENEWABLE ENERGY DISTRIBUTED POWER SYSTEMS

Per Karlsson and Jörgen Svensson
Department of Industrial Electrical Engineering and Automation, Lund University
Box 118
S-221 00 Lund
Sweden

ABSTRACT

This paper addresses voltage control of distributed DC power systems. Especially the dynamic properties of load-source interactions are highlighted. They are interesting since the sources are considered weak for a distributed power system. This is illustrated with simulations where the power is fed from wind turbines only, and still constant power loads are controlled at the same time as the DC bus voltage level. The wind power generators are modeled as permanent magnet synchronous machines. The controller needed for the machines, including position estimation and field weakening, is discussed. To control the DC bus voltage, more power than consumed by the loads must be supplied to the wind turbines and the excess power removed by pitch angle control. Pitch angle control is a comparably slow process and therefore the DC bus voltage controller must handle the transient power distribution.

KEY WORDS

DC distribution system, distributed generation, droop control, wind energy.

1. INTRODUCTION

This paper investigates source-load interaction for a DC distributed power system based on renewable energy sources. The main issue investigated is the DC bus voltage control when applied to a wind powered system.

Several different DC bus voltage control schemes exist [1], where especially two seem commonly used; master-slave and droop control [2]. The master-slave method strongly relies on fast communication between the source and load converters. One of the converters, referred to as the master, is responsible for controlling the DC bus voltage and distributing power references to the other converters. The method used in this paper, is referred to as voltage droop control. Droop control does not require any communication between the converters. Instead, the DC bus voltage is measured at each source converter. All the source converters give power contributions to balance the total power consumed by the loads and the losses of the DC power system. In common voltage droop control the DC bus voltage reference declines linearly as the output current, or in some cases power, for the converter increases, in order to give stable operation. This, of course, gives a stationary error in the voltage level. The voltage droop controller used in this paper is further developed to include droop offset control acting dynamically on wind turbine speed variations.

The paper begins with an overview of the structure of the investigated DC distributed power system. Then the controller structures and suitable parameters are given. Last, some simulation results are discussed.

2. DC POWER DISTRIBUTION

The investigated DC distribution network model consists of five converters (Fig. 1) where three are operated as sources and two are feeding power to loads. The converters are connected to electrically separated AC power sources or loads, i.e. without common reference or ground, as a result of the neutral voltage shift problems discussed in [3].

To investigate the transient response of the DC bus voltage controllers, the power references for the power fed to the loads are changed in steps. Therefore, the dynamics of the energy sources interfere with the dynamics of the voltage control, which is further discussed later.
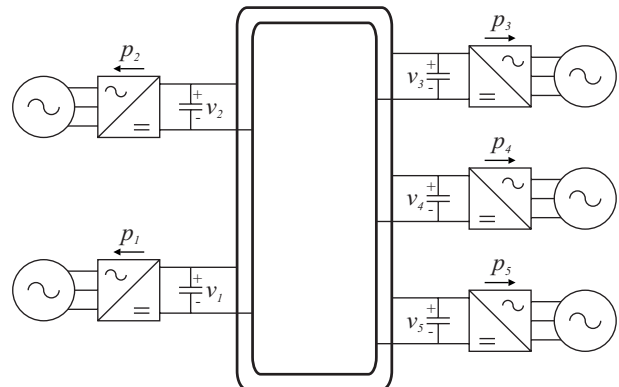
Fig. 1.   The investigated DC power system configuration.

The controller structure for the DC bus voltage control is shown in Fig. 2. A proportional (P) controller is used for the

droop scheme, similar to the PI-controller derived in [4] for back-to-back converter DC link voltage control. This controller structure should be implemented in all converters, intended for DC bus voltage control. The reason for this is to distribute the total load between as many converters as possible when droop control is used. The measured DC bus voltage is low-pass filtered (Fig. 2) to attenuate the interaction between the negative sequence voltage of the AC side and the DC bus voltage control discussed in [4] and to enhance controller pole placement.
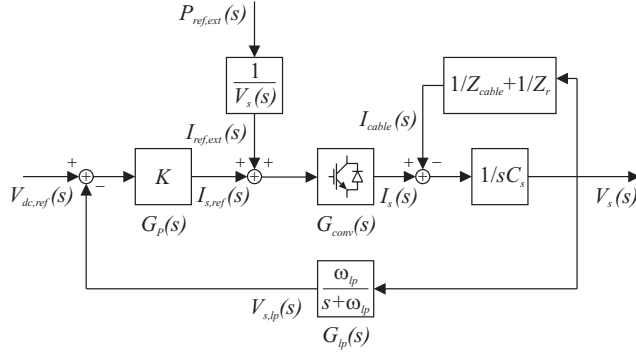
Fig. 2. Control structure for DC bus voltage control. The source converter current is denoted I_s and the cable current I_{cable}.

The DC bus voltage controller for the droop scheme is a P-controller with gain K. In the case of a single source and receiver this gives a droop function according to

$$V_s(s) = \frac{(K/C_{dc})(s+\omega_{lp})}{s^2 + \omega_{lp}s + \omega_{lp}(K/C_{dc})} V_{dc,ref}(s) - \frac{(1/C_{dc})(s+\omega_{lp})}{s^2 + \omega_{lp}s + \omega_{lp}(K/C_{dc})} I_r(s)$$

(1)

where I_r is the receiving end current and C_{dc} the total DC link capacitance including the cable. The DC link capacitor of each converter, both sending and receiving, is selected according to

$$C_{dc,converter} = \frac{P_n}{V_{dc,ref}^2} \cdot \frac{2\zeta_n^2}{\omega_{lp}} \cdot \frac{1}{(1-\delta_n)\delta_n}$$

(2)

to give equivalent behavior of the source converters in per unit. Note that for a multi-converter system all the source converters should have the same stationary characteristic in order to obtain a proper load sharing. This is fulfilled if the DC side capacitor of each converter is selected according to the expression above. Furthermore, for an ideal cable, i.e. without any impedance other than the DC side capacitors, the system transfer function will be the same as for a two-converter system. For a system with a reference DC voltage of $V_{dc,ref}$=750 V, break over frequency of the low-pass filter given by ω_{lp}=2π30 rad/s, a droop function damping equal to ζ_n=0.707, and a voltage droop at rated load equal to δ_n=0.05, each converter should have a DC side capacitance to rated power ratio of 199 μF/kW.

3. WIND POWERED DC BUS

Wind power is one of the most promising renewable energy sources. The reasons for this are, for example, high efficiency also for the present wind power technologies and the fact that wind power turbines can be located on-shore and off-shore with high power production even for relatively small installations. Another benefit is that the rotating mass constitutes an energy storage, which means that small wind variations might not disturb the power transfer significantly. The excess power fed to the wind turbines is removed by pitch angle control, explained below. The problem in this case is that the turbine speed will increase which might result in severe mechanical stress and an increased back-emf of the generators. Most modern wind power turbines are speed controlled by means of pitch angle control. However, the pitch angle control has a rather low bandwidth, with time constants in the range of seconds.

First it is investigated how the DC distribution system responds to a sudden block of the load converters, e.g. before pitch angle control is fully established. The pitch angle is controlled in such a way that the steady state mechanical power delivered to the generator is expressed as

$$\begin{cases} P_{gen} = P_{wind} - P_{pitch} \\ P_{wind} = K_{wind} v_{wind}^3 \end{cases}$$

(3)

where v_{wind} is the wind speed. The power lost due to pitch angle control is given by

$$P_{pitch} = K_{pitch} \left(\omega_{m,ref} - \omega_m\right)$$

(4)

where ω_m is the mechanical speed. The gain is found from the time constant τ_{pitch} and the moment of inertia J_m

$$K_{pitch} = -\omega_m \frac{J_m}{\tau_{pitch}} \cdot \frac{P_{wind}}{P_n}$$

(5)

For transients, the following differential equation applies

$$J_m \frac{d\omega_m}{dt} = \frac{P_{wind} - P_{pitch} - P_{gen}}{\omega_m}$$

(6)

Assuming the initial conditions

$$\begin{cases} P_{wind}(t_0) = P_0 \\ P_{gen}(t_0^-) = P_0 \end{cases} \text{ and } \begin{cases} P_{wind}(t_0) = P_0 \\ P_{gen}(t_0^+) = 0 \end{cases}$$

(7)

the following expression is approximately valid for the pitch angle controller

$$P_{pitch} = P_0 \left(1 - e^{-(t-t_0)/\tau_{pitch}}\right)$$

(8)

which gives the following differential equation

$$\omega_m \frac{d\omega_m}{dt} = \frac{P_0}{J_m} e^{-(t-t_0)/\tau_{pitch}} \tag{9}$$

with the solution

$$\frac{1}{2}\omega_m^2 = P_0 \frac{\tau_{pitch}}{J_m}\left(1-e^{-((t-t_0)/\tau_{pitch})}\right)+\frac{1}{2}\omega_{m0}^2 \tag{10}$$

where ω_{m0} is the mechanical speed at time t_0. Thus, the stationary mechanical speed is given by

$$\omega_{m,stat} = \sqrt{2P_0\frac{\tau_{pitch}}{J_m}+\omega_{m0}^2} \tag{11}$$

The worst-case increase is when operating at rated (index n) speed and power, i.e.

$$\Delta\omega_{m,max} = \omega_{m,stat,max}-\omega_{m,n} = \sqrt{2P_n\frac{\tau_{pitch}}{J_m}+\omega_{m,n}^2}-\omega_{m,n} \tag{12}$$

From (12) a droop offset control gain used to divide the wind power between the source converters is given by

$$K_\omega = -\frac{\Delta V_{dc,ref,max}}{\Delta\omega_{el,max}} = -\frac{(1-\delta_n)\delta_n V_{dc}}{\sqrt{2P_n\frac{\tau_{pitch}}{J_m}z_p^2+\omega_{el,n}^2}-\omega_{el,n}} \tag{13}$$

where z_p is the number of pole pairs for the electric machine and ω_{el} is the electrical angular frequency. A new DC bus voltage reference is formed

$$V_{dc,ref} = V_{dc,ref0} + K_\omega\left(z_p\omega_{m,ref}-\hat{\omega}_{el}\right) \tag{14}$$

where $V_{dc,ref0}$ is the initial reference, equal to the no-load DC bus voltage. Thus, the droop characteristic is shifted up- or down-wards, depending on the difference between the speed reference and the estimated electrical speed.

A permanent magnet synchronous machine (PMSM) is suitable for wind power applications for two reasons. Firstly, if a multiple pole generator, i.e. a machine with low mechanical base speed, is used the mechanical gearbox can be omitted. Secondly, the most suitable machine for low base speed is the PMSM, at least compared to other three phase machines, e.g. the induction machine.

A current controller similar to the one used for AC network connected converters [4] is needed for the control of a PMSM. However, the PMSM of a single wind turbine cannot be regarded as a stiff power source, which means that the frequency is far from constant. The speed and position need to be estimated to fix the rotating dq-coordinate system [4] and to calculate the reactive voltage drop fed forward in the current controller. To track the speed variations, a speed and position estimator is needed. The one used here is based on the results obtained in [5].

First the d-direction back-emf e_d is estimated

$$e_{d,k} = v_{d,k}-R_s i_{d,k}^{ref}-\hat{\omega}_{el,k-1}L_q i_{q,k}^{ref} \tag{15}$$

where R_s is the stator resistance and L_q the stator inductance in the q-direction. The angular frequency is estimated from

$$\hat{\omega}_{el,k} = \hat{\omega}_{el,k-1}-T_s\gamma_1\left(\omega_{f,k}\right)e_{d,k} \tag{16}$$

where T_s is the sampling interval. The angular position is estimated from

$$\hat{\theta}_k = \left[\hat{\theta}_{k-1}+T_s\hat{\omega}_{el,k-1}-T_s\gamma_2\left(\omega_{f,k}\right)e_{d,k}\right]_0^{2\pi} \tag{17}$$

The estimated speed is low-pass filtered according to

$$\omega_{f,k} = \omega_{f,k-1}+T_s\rho_s\left(\hat{\omega}_{el,k-1}-\omega_{f,k-1}\right) \tag{18}$$

which is then used to calculate suitable adaptation gains [5]

$$\begin{cases} \gamma_1 = \dfrac{\rho_0^2}{\omega_f\Psi_m}\cdot z_p \\[4mm] \gamma_2 = \dfrac{2\rho_0}{\omega_f\Psi_m}\cdot z_p \end{cases} \tag{19}$$

where Ψ_m is the flux linkage and ρ_0 the real valued double pole of the estimator. According to [5] a proper choice is

$$\rho_0 = \sqrt{\rho_s 0.2\cdot\omega_{el,n}/\sin(5°)} \tag{20}$$

where ρ_s is the bandwidth of the speed control loop. In this application, the speed is not actually controlled. Instead an internal droop offset is created from the speed deviation. Since the speed varies slowly in a wind power application, a bandwidth of 10 Hz ($\rho_s=2\pi10$ rad/s) should be sufficient.

When the load converters are blocked, the speed might increase to a level considerably higher than base speed. The induced back-emf, $e_q=\omega_m\Psi_m$, might reach so high levels. that the controlled transistor converter starts to act as a non-controlled diode rectifier, formed by the freewheeling diodes. Field weakening is introduced to circumvent this potential risk. In field weakening, reactive power is consumed so that the machine terminal voltage is kept at the average level

$$v_q = R_s i_q + \omega_{el}L_d i_d + e_q \tag{21}$$

A control law could be formed directly from this expression. However, this would give a high gain and since the speed is estimated, result in an oscillatory behavior. Therefore, the d-component of the current is filtered with a first order low-pass filter with $\omega_{p,id}=\rho_s/10$. Then the difference between the back-emf at rated speed and the estimated back-emf minus the estimated field-weakening component is fed to a PI-controller, see Fig. 3.
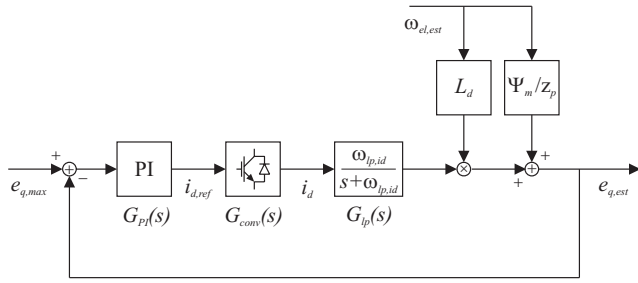
Fig. 3. Controller structure for generation of the d-current reference used for field weakening action. Note that the machine back-emf is estimated.

The gain and integrator time constant of this PI controller is selected in such a way that the closed loop poles of the field weakening subsystem, are given by

$$\rho_{1,2} = -(2\alpha_{id} - 1)\omega_{lp,id} \qquad (22)$$

assuming that the speed estimation is correct. In (22), α_{id} is a weighting factor to reduce the gain of the field weakening subsystem. A suitable value is $\alpha_{id}=0.55$. The gain and integrator time constants used to generate the d-current reference needed for field weakening are given by

$$\begin{cases} K_f = (2\alpha_{id} - 1) \cdot \dfrac{1}{L_d} \cdot \left(\dfrac{\Psi_m}{z_p} + \dfrac{1}{|\omega_{el}|} \right) \\[2mm] T_{if} = \dfrac{1}{\omega_{lp,id}} \cdot \dfrac{2\alpha_{id} - 1}{\alpha_{id}^2} \end{cases} \qquad (23)$$

for a continuous time controller. A sampled controller is used in the simulation and therefore the controller is transformed by backward Euler-transformation.

4. SIMULATIONS

Load sharing and load converter blocking are investigated in simulations. A ring bus network configuration [2] (Fig. 1) is used for the study. Each cable segment between two converters is modeled as a π-link with series resistance R=64.7 mΩ, series inductance L=52.7 μH and parallel capacitance C=5.27 nF. To calculate an appropriate cable resistance, it is assumed that the cable length of each segment is 100 m and that the maximum current density is 4 A/mm^2 even if the ring bus is broken. The latter assumption is made since a cable segment might be disconnected during a fault. The cable inductance is calculated assuming a distance between the centers of the conductors equal to twice the conductor diameter. The converter and AC side parameters are given in Table I. The parameters for the wind power aggregates, connected to converter 1, 3 and 5, are set to

$$\begin{cases} J_m/P_n = 40 \, \text{kgm}^2/\text{kW}, \ z_p = 40 \ \Leftrightarrow \ H = 1.2 \, \text{s} \\ \tau_{pitch} = 1 \, \text{s} \end{cases} \qquad (24)$$

Table I   Simulation model data.

Converter no.	1	2	3	4	5
P_n [kW]	25.0	100.0	50.0	50.0	75.0
$E_{LN,RMS,n}$ [V]	400	400	400	400	400
$f_{elec,n}$ [Hz]	50	50	50	50	50
f_{sw} [kHz]	7.5	7.5	4.95	5.0	4.95
L_d [mH]	9.78	1.50	4.89	3.00	3.26
L_q [mH]	9.17	1.50	4.58	3.00	3.06
R_s [Ω]	0.5	0.25	0.5	0.25	0.5
C_{dc} [mF]	5.0	20.0	10.0	10.0	15.0
$V_{dc,ref}$ [V]			750		

The speed reference is maintained at $\omega_{m,ref}$=6.23 rad/s throughout all the simulations. The power fed to the wind turbines equals rated power (P_n). The moment of inertia used for the simulations is approximately five times lower than for real aggregates. The reason to select such a low moment of inertia is to make the source more weak, with higher speed variations, in order to investigate the controller operation. The system has been simulated with five times higher moment of inertia and it is found that the result is similar except that the speed variations are five times lower.

Three cases are studied. First wind speed variations are considered. Second, load sharing is investigated. Third, a load converter block situation is considered. In all three cases, the investigation starts at a condition where the load converters are loaded to half their rated power, respectively. For an ideal system, i.e. with zero cable impedance, the source converters should also be loaded to half their rated power. For a realistic system, including cable impedance, it is cumbersome to determine the maximum allowable load converter output power for a given wind situation by analytical methods. However, the actual loading of each source converter can be calculated with a load flow program, similar to the ones used for AC system analysis, to give the input power needed for a certain loading.

In the figures shown in this section, black curves denote source converter quantities and grey denotes load converter quantities. Quantities belonging to converter subsystem 1 are solid black, 2 are solid grey, 3 are dashed black, 4 are dashed grey, and 5 are dash-dotted black.

From the initial operating point introduced above, the wind speed at converter 1 suddenly drops at t=0.5 s, resulting in a wind turbine input power reduction from rated level (25 kW) to 40% of rated power (10 kW). Consequently, the two other source converters (3 and 5) are more heavily loaded (Fig. 4). The increased loading of the converters 3 and 5 result in a decreased DC bus voltage, due to droop control action. The power delivered from converter 1 is reduced since the droop offset control reduces $V_{dc,ref}$ for this converter. Thus, the voltage error decreases and the power delivered via converter 1 is reduced. Fig. 5 shows the

DC bus voltages at the converters. The power removed by pitch angle control for wind power aggregate 1 is shown in Fig. 6. Note that the power removed by pitch angle control drops suddenly at t=0.5 s due to the rapid decrease in input power. Both the droop offset controller and the pitch angle controller rely on an external speed reference. This reference is based on actual wind speed and power delivering capability and assumed being supplied from a supervisory controller used for the entire DC distributed power system. The speed references are not altered during the simulation.
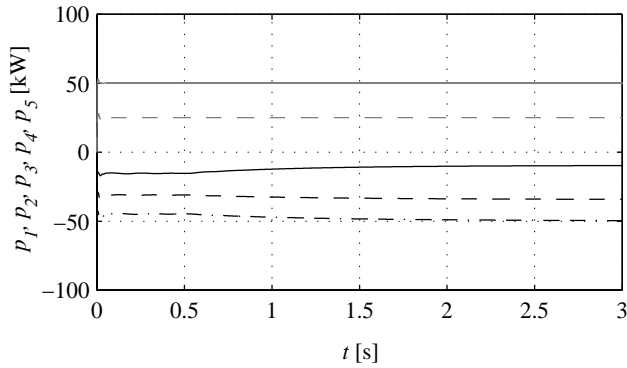
Fig. 4. Converter DC side power for converter 1 to 5 at a wind power decrease of 15 kW (60% of rated power) at t=0.5 s for converter 1 starting from 25 kW (rated power).
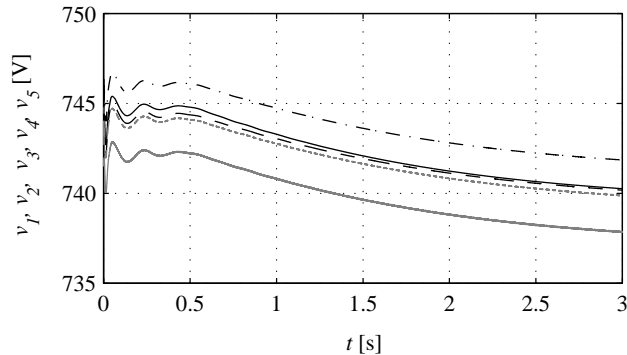
Fig. 5. DC bus voltage levels at the converter DC terminals.
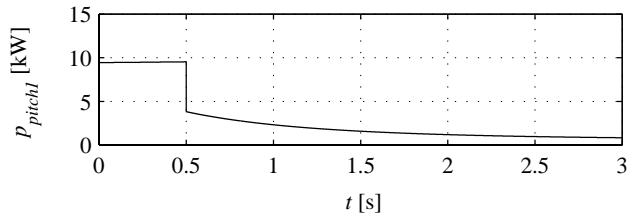
Fig. 6. The power removed at wind turbine 1 due to pitch angle controller action.

From the initial operating point, the output power of converter 2 increases by 10% of rated power at t=0.5 s and the output power of converter 4 increases by 10% of rated power at t=1.0 s (Fig. 7). In Fig. 7 it is shown that the load sharing works properly both in transient and stationary conditions. The DC bus voltage level at each converter

terminal is shown in Fig. 8. Note the rapid steps in DC bus voltage seen in Fig. 8 when the output power is changed. These are caused by the droop control action. The slow variation in DC bus voltage is due to internal droop offset adjustment caused by the speed error resulting from the reduced actual speed.
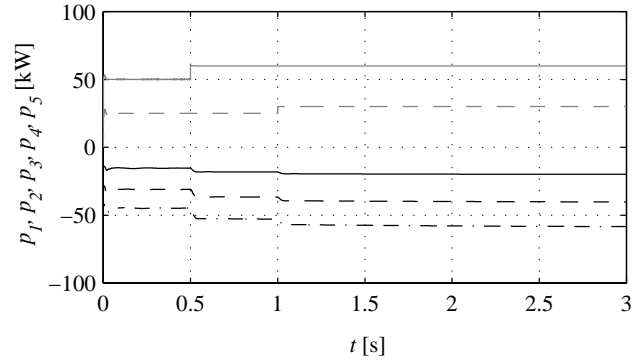
Fig. 7. Output power increase of 10% of rated load converter power at t=0.5 s for converter 2 and 1.0 s for converter 4 starting from 50% of rated power for both converters.
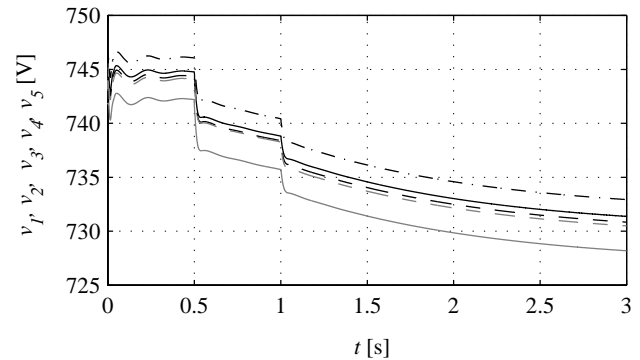
Fig. 8. DC bus voltage levels at the converter DC terminals.

From the initial operating point, converter 2 is blocked, i.e. its output power is decreased to 0, at t=0.5 s and converter 4 is blocked at t=1.0 s (Fig. 9). As illustrated in Fig. 9, load sharing works properly also in this case. Fig. 10 shows the corresponding DC bus voltages at the converter terminals. Again, they exhibit both rapid and slow variations. Note that the DC bus voltages approach each other as the loading decreases due to the reduced resistive voltage drop experienced at light load. The actual and estimated electrical speed for converter subsystem 1 is shown in Fig. 11. It is clearly seen that the bandwidth of the speed estimator is sufficient.

Fig. 12 shows the d- and q-currents for converter subsystem 1. The corresponding references are not shown since the current components track their respective reference. The d-current reference becomes negative due to the fact that the speed becomes higher than the base speed. The q-current reference is a measure of the active power delivered to the AC side of the converter. Since the power is delivered from the AC side to the DC side of converter subsystem 1, the initial q-current reference is negative.
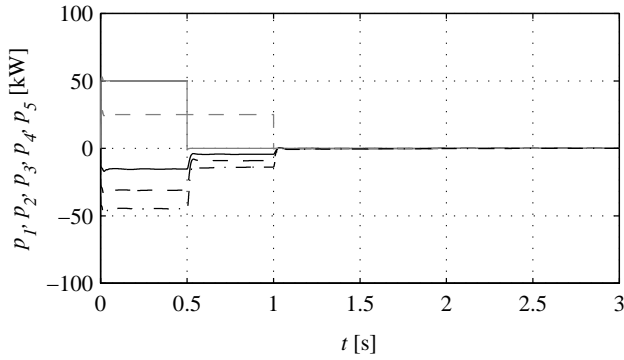
Fig. 9. Output power decrease of 50% of rated load converter power at t=0.5 s for converter 2 and 1.0 s for converter 4 starting from 50% of rated power for both converters.
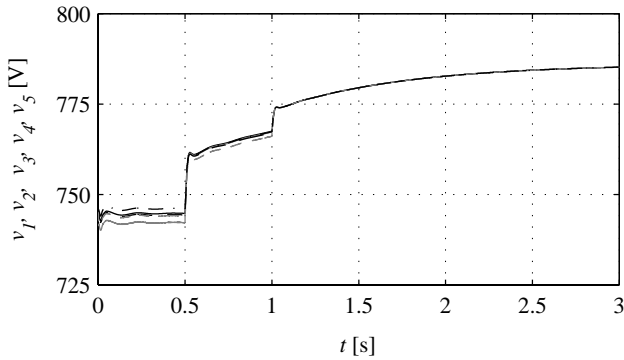
Fig. 10. DC bus voltage levels at the converter DC terminals.
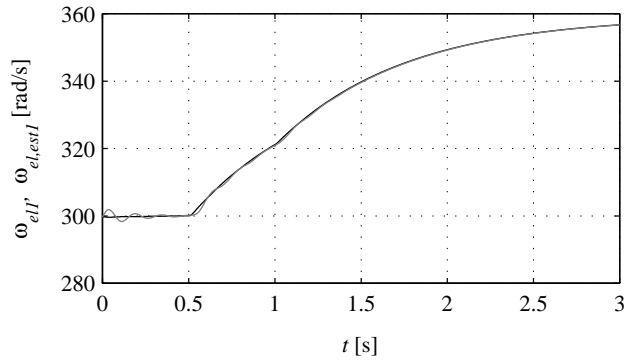
Fig. 11. Actual (black) and estimated (grey) electrical speed for the wind turbine connected to converter 1.
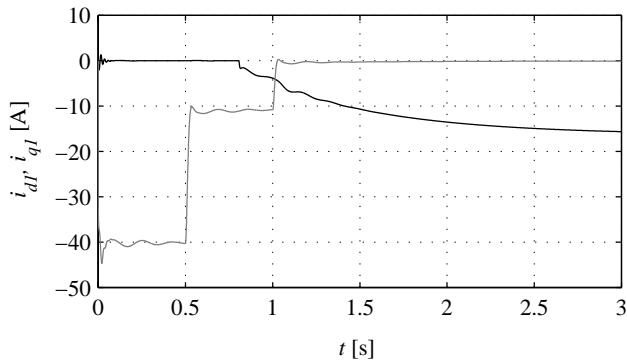
Fig. 12. The *d*- (black) and *q*-current (grey) components for converter 1.

5. CONCLUSIONS

In this paper it is shown that a DC distributed power system with converters specified according to (2), can be operated with only wind power turbines as power sources. The investigated droop control scheme used is further developed to include droop offset control to handle wind power variations. The droop offset controller acts to reduce the power drawn from wind turbines operating at lower power than expected. The sources and loads operate as autonomous units, which means that high-speed communication is not needed. The updating of the externally calculated turbine speed references could be of low-speed type, which is reflected by the fact that they are not updated during the simulations. The only demands are that the power fed to the turbines should exceed the power fed to the loads, including the losses, and that the wind turbine aggregates should be equipped with pitch angle control. The simulation results verify that moderate disturbances as well as extreme variations are handled properly.

6. ACKNOWLEDGMENT

REFERENCES

[1] S. Luo, Z. Ye, R.-L. Lin and F.C. Lee, A classification and evaluation of paralleling methods for power supply modules, *IEEE-PESC Conf. Rec.*, PESC '99, Charleston, SC, USA, 1999, 901-908.

[2] W. Tang and R.H. Lasseter, An lvdc industrial power distribution system without central control unit, *IEEE-PESC Conf. Rec.*, PESC '00, Galway, Ireland, 2000, 979-984.

[3] K. Xing, F.C. Lee, J.S. Lai, G. Thandi and D. Borojevic, Adjustable speed drive neutral voltage shift and grounding issues in a dc distributed power system, *IEEE-IAS Conf. Rec.*, IAS '97, New Orleans, LA, USA, 1997, 517-524.

[4] M. Bojrup, *Advanced control of active filters in a battery charger application* (Lund, Sweden, Department of Industrial Electrical Engineering and Automation, Lund Institute of Technology, 1999).

[5] L. Harnefors, *On analysis, control and estimation of variable-speed drives* (Stockholm, Sweden, Department of Electric Power Engineering, Royal Institute of Technology, 1997).